Identification of electromechanical coupling in piezo-structures

Pascal De Boe[(1)], Jean-Claude Golinval[(2)]

LTAS – Vibrations et Identification des Structures,
Université de Liège, B-4000 Liège, Belgium.
[(1)] pdeboe@ulg.ac.be, [(2)] jc.golinval@ulg.ac.be, http://isis.ulg.ac.be

Abstract

An identification method based on a structural model updating procedure may be used to improve the knowledge of a piezoelectric tested structure and to determine the coupling coefficients of the piezoelectric material. This procedure starts with the modal analysis of the open-loop instrumented structure. Let the target modes be a subset of the model modes; a selection of sensor (generally accelerometers) locations is then performed by determining the smaller subset such that the H_2 modal norm is as close as possible to the modal norm of the original full set. In most cases, experimental testing with the selected sensor set will give acceptable information to identify target modes. These data, coupled with electrical sensing at the piezoelectric element level, will then be used to perform modal analysis of the piezo-structure. A pole-residue development of the open-loop piezo-structure shows that conventional algorithms may be used to estimate the mechanical modal parameters and the electromechanical coupling matrix.

The second step of the procedure is to perform model updating itself. The initial finite element piezoelectric model will be improved stiffness corrections to the global stiffness matrix.. The corrections are split in their mechanical and electromechanical contributions. It is then possible to separate mechanical modelling errors from electromechanical coupling errors. The problem becomes a classical model updating problem which may be solved using well established techniques. This will result not only in a model behaving like the measures, but also in an improved knowledge of the structure behaviour without loosing physical insight. From a numerical point of view, it will be shown that ill-conditioning inherent to the presence of piezoelectric elements presents some difficulties at different steps of the model correction procedure.

A clamped-free plate instrumented with piezo-laminates is used to illustrate the model updating approach. The selection of measurement points, using the modal norm criteria, is also presented. Experimental identification data will then be used as inputs for the model correction procedure and the behaviour of the updated model will be compared with the initial model dynamics.

Introduction

The general trend to design light-weight structures is generally antagonist to the mechanical requirement in term of vibrational stability and accuracy. Active control of such flexible structures is a solution to overcome this problem. Modelling field, which use often the finite elements method (*FEM*), has then been improved in order to have a satisfactory prediction of the dynamic. The performances of the model is important because it could condition the ability of an implemented active system to follow the dynamic behaviour of the actual structure. Unfortunately, a numerical model contains some uncertainties inherent to the boundary conditions and to the physical properties of structural materials. Errors are also induced by the discretisation and by the condensation of the actual structural degrees of freedom to an acceptable size for the controller.

A model correction procedure, called model updating, could be then useful in order to improve the structural dynamic prediction. One way is to correct the estimated masses and stiffness . The idea is then to update the initial model in order to minimise the distance between the numerical prediction and the measured data; whether in the modal or frequency domain.

Literature exhibits several hundred papers on the model updating of conventional 'passive' structures. Maia and al. summarise the various published techniques in this field, but none of them are applied on '*smart*' structures. This paper will show the application of the frequency domain updating technique on '*smart*' structures fitted with piezoelectric elements.

Piezoelectric elements are very popular in the field of active control. Their light-weight and distributed properties are very attractive to overcome the structural vibration suppression challenge. There are two fundamental electromechanical effects associated with piezoelectricity, namely the direct effect and the converse effect. Direct effect can be detected when applying a force on a piezoelectric material and monitoring the electrical voltage or charge generated. Inversely, to emphasise the converse effect, an electric field can be applied to the material which will induce stress or strain. Piezoelectricity is used for a large number of applications in the field of electromechanical engineering, e.g. waves-sound generators, echo-graphic probes, micro-positioner, accelerometer transducers, pressure transducers,... Thin

piezoelectric laminates are widely used as distributed sensors and distributed actuators and are very well adapted for the control of elastic shells or plates.

Modal analysis of a piezo-structure

The modal testing of a structure fitted with distributed piezo-electric sensor/actuator is described by Saunders and al.. The pole-residue model is developed by reminding the modal decomposition of a viscously damped and linear passive structure :

$$\mathbf{M} \cdot \ddot{\mathbf{x}} + \mathbf{D} \cdot \dot{\mathbf{x}} + \mathbf{K} \cdot \mathbf{x} = \mathbf{f} \qquad (1)$$

with
- $\mathbf{M}$ *n x n* mass matrix, symmetric and definite positive,
- $\mathbf{D}$ *n x n* damping matrix,
- $\mathbf{K}$ *n x n* stiffness matrix, symmetric and definite positive,
- $\mathbf{f}$ *n x 1* vector of structural forces,
- $\mathbf{x}$ *n x 1* vector of structural degrees of freedom.

The resolution of the eigenvalues problem associated with (1) yields *n* pairs of complex conjugate eigenvalues :

$$\mathbf{p_i} = -\zeta_i \cdot \omega_i \pm \mathbf{j} \cdot \omega_i \cdot \sqrt{1 - \zeta_i^2} \qquad \mathbf{i} = 1, 2, \ldots \mathbf{n} \qquad (2)$$

associated with *n* complex eigenvectors Φ (*nxn*). In the case of proportional or diagonal damping the $\mathbf{p_i}$ eigenvalues are linked to the solutions ω_i of the associated non-damped system and with the modal critical damping ζ_i (see Géradin and Rixen).

For a force applied at the spatial position $\mathbf{l}$ and for a response measured at the spatial position $\mathbf{k}$, the frequency response function (***FRF***) is expressed by :

$$\frac{\mathbf{x_k}}{\mathbf{f_l}} = \alpha_{kl} = \sum_{i=1}^{n} \left\{ \frac{\phi_{ki} \cdot \phi_{li}}{\mathbf{m_i} \cdot \left[\mathbf{j} \cdot \omega - \mathbf{p_i} \right]} + \frac{\phi_{ki}^{*} \cdot \phi_{li}^{*}}{\mathbf{m_i} \cdot \left[\mathbf{j} \cdot \omega - \mathbf{p_i}^{*} \right]} \right\} \qquad (3)$$

with $\mathbf{m_i}$ the modal mass associated with the ith mode ϕ_i .

In the case of a structure fitted with a piezoelectric sensor/actuator, electromechanical relationship are added to the previous system of equations of motion (1) to represent contributions of the electrical degrees of freedom linked to the piezoelectric actuator and sensor :

$$\begin{aligned} \mathbf{M} \cdot \ddot{\mathbf{x}} + \mathbf{D} \cdot \dot{\mathbf{x}} + \mathbf{K} \cdot \mathbf{x} &= \mathbf{f} + \Theta^{a} \cdot \mathbf{v}_{a} \\ \Theta^{s^{T}} \cdot \mathbf{x} + \mathbf{C}_{p} \cdot \mathbf{v}_{s} &= \mathbf{q} \end{aligned} \qquad (4)$$

The first equation is commonly called the actuator equation and the second, the sensor equation. The actuator equation exhibits the force generated by the piezoelectric actuator through the electromechanical coupling actuator matrix Θ^{a} and the electrical potentials applied at each electrodes of the elements. On the other hand, the sensor equation shows the relationship existing between the mechanical degrees of freedom $\mathbf{x}$ and the electrical charges $\mathbf{q}$ or potentials $\mathbf{v}_s$ through the electromechanical coupling matrix $\Theta^{s^{T}}$ and the capacitance $\mathbf{C}_p$ of sensor.

In the case of a force applied on a system only fitted with a piezoelectric sensor, and by forcing the electrode potentials to zero with a short-cut (e.g. : physically, by means of a perfect charge amplifier), we can write :

$$\begin{aligned} \mathbf{M} \cdot \ddot{\mathbf{x}} + \mathbf{D} \cdot \dot{\mathbf{x}} + \mathbf{K} \cdot \mathbf{x} &= \mathbf{f} \\ \Theta^{s^{T}} \cdot \mathbf{x} &= \mathbf{q} \end{aligned} \qquad (5)$$

The first thinks to observe is that the presence of the piezoelectric sensor don't modify the dynamic behaviour of the structure (same eigen-frequencies, modes and modal critical damping and masses). On the other hand, remembering (3), it is easy to find the relation between the electrical sensing and the applied force decomposed in a summation of modal participation weights :

$$\frac{\mathbf{v}_s}{\mathbf{f}_l} = \sum_{i=1}^{n} \left\{ \frac{\Theta^{s^{T}} \cdot \phi_i \cdot \phi_{li}}{\mathbf{m}_i \cdot \left[\mathbf{j} \cdot \omega - \mathbf{p}_i \right]} + \frac{\Theta^{s^{T}} \cdot \phi_i^{*} \cdot \phi_{li}^{*}}{\mathbf{m}_i \cdot \left[\mathbf{j} \cdot \omega - \mathbf{p}_i^{*} \right]} \right\} \qquad (6)$$

This last relation is very important because it induces that the determination of the electromechanical coupling matrix is theoretically possible by means of an experimental modal analysis and an adequate set of measurements.

Extraction of the modes, eigen-frequencies, modal damping and masses could be performed with conventional modal analysis algorithms applied on experimental structural **FRF** s. Note that correct estimation of modes needs measurement at a driving point, i.e. where excitation and response are measured at the same position and in the same direction (see Maia, Silva and al.).

Once dynamic parameters extracted, it is easy, by (6), to retrieve the electromechanical coupling matrix Θ^{s^T} . Estimation of the actuator electromechanical coupling matrix Θ^a can also be estimated with the same method by simply using the actuator in sensor mode. Unfortunately, complete estimation of Θ^{s^T} is only possible if all mechanical degrees of freedom in common with the piezoelectric element are monitored, which could be practically difficult. This implies that the knowledge of the piezoelectric elements will be only partial unless a structural model (generally a finite element model which contains errors due to simplifications and material uncertainties), improved by experimental data, is available. The structural model improvement (namely : model updating) will depends of the selected frequency range (it is obviously false to believe that an updated model will be valid from 0 Hz to ∞ Hz) and of the quality of the available measurements. It is then important that experimental data set is rich enough to afford a correct identification of all the modes existing in the selected frequency range of interest.

Excitation and measurement points selection for experimental modal analysis

The selection of the optimal positions of excitation and sensing is not a simple task. Without any criteria, engineer judgement and various trials are needed to obtain an acceptable set of data able to perform a correct identification of modes in the frequency range of interest. This procedure is time-consuming and not very effective. The problem of actuator and sensor placement have been already investigated in literature. Kammer proposes the selection of the best signal to noise ratio position. In Gawronski, the procedure is based on the monitoring of the observability and controllability Grammians to choose optimal excitation and sensor locations.

Controllability is a means to measure the ability of a particular excitation configuration to control all the states of the system : if it is possible to transfer the state of a system $\mathbf{x}(0)$ to its origin $\mathbf{x}(t_1) = 0$ with t_1 finite. Conversely, observability measures the ability of a sensor configuration to estimate all the states of a system : if it is possible to determine the state of system $\mathbf{x}(t_1)$ from the sensor configuration $\mathbf{y}(t)$, $t \in [t_0, t_1]$ and where t_1 is a finite time.

To apply the theory of controllability and observability, which has been developed in the theory of control, it is convenient to express the

generalised (multi-excitations and outputs) system nodal representation (1) in the form :

$$\begin{aligned} \mathbf{M}\cdot\ddot{\mathbf{x}} + \mathbf{D}\cdot\dot{\mathbf{x}} + \mathbf{K}\cdot\mathbf{x} &= \mathbf{B}_0\cdot\mathbf{f} \\ \mathbf{y} &= \mathbf{C}_{0x}\cdot\mathbf{x} + \mathbf{C}_{0\dot{x}}\cdot\dot{\mathbf{x}} \end{aligned} \qquad (7)$$

where $\mathbf{y}$ is defined as the output vector and depends linearly of the structural displacements and velocity.
The state space-form can be written then :

$$\begin{aligned} \dot{\aleph} &= \mathbf{A}\cdot\aleph + \mathbf{B}\cdot\mathbf{f} \\ \mathbf{y} &= \mathbf{C}\cdot\aleph \end{aligned} \qquad (8)$$

where we define :

$$\aleph = \begin{Bmatrix} \mathbf{x} \\ \dot{\mathbf{x}} \end{Bmatrix} \qquad (9)$$

the state-space vector of size $\mathbf{N} = 2\cdot\mathbf{n}$ which includes the system displacements and velocities. Elementary manipulations link the expression of the system nodal representation (1) to the nodal sate space form (8) :

$$\mathbf{A} = \begin{bmatrix} 0 & \mathbf{I} \\ -\mathbf{M}^{-1}\cdot\mathbf{K} & -\mathbf{M}^{-1}\cdot\mathbf{D} \end{bmatrix} \quad \mathbf{B} = \begin{bmatrix} 0 \\ \mathbf{M}^{-1}\cdot\mathbf{B}_0 \end{bmatrix} \quad \mathbf{C} = \begin{bmatrix} \mathbf{C}_{0x} & \mathbf{C}_{0\dot{x}} \end{bmatrix} \qquad (10)$$

In classical control theory (see Kwakernaak and Sivan), a linear time invariant system $(\mathbf{A},\mathbf{B},\mathbf{C})$ is fully controllable if and only if the constructed matrix :

$$\mathbf{C} = \begin{bmatrix} \mathbf{B} & \mathbf{A}\cdot\mathbf{B} & \mathbf{A}^2\cdot\mathbf{B} & \dots & \mathbf{A}^{N-1}\cdot\mathbf{B} \end{bmatrix} \qquad (11)$$

has rank $\mathbf{N}$. In the same way, a linear time invariant system $(\mathbf{A},\mathbf{B},\mathbf{C})$ is fully observable if and only if the matrix :

$$\mathbf{O} = \begin{bmatrix} \mathbf{C} \\ \mathbf{C}\cdot\mathbf{A} \\ \vdots \\ \mathbf{C}\cdot\mathbf{A}^{N-1} \end{bmatrix} \qquad (12)$$

has rank N. As clearly explained in Gawronski, these criteria, although simple, are not at all efficient :

- the level of controllability or observability is not quantified; but only give an answer in term of yes or no.
- The computation of $\mathbf{C}$ or $\mathbf{O}$ is prohibitive in case of system with realistic size.

These two drawbacks bring us to prefer expressing the system properties in term of Grammians. The controllability and observability Grammians are defined as follows :

$$\mathbf{W_c}(t) = \int_0^t e^{\mathbf{A}\cdot t} \cdot \mathbf{B} \cdot \mathbf{B}^T \cdot e^{\mathbf{A}^T \cdot t}\, dt \qquad \mathbf{W_o}(t) = \int_0^t e^{\mathbf{A}^T \cdot t} \cdot \mathbf{C}^T \cdot \mathbf{C} \cdot e^{\mathbf{A}\cdot t}\, dt \quad (13)$$

The controllability grammian reflects the ability of a perturbation $\mathbf{f}$ to perturb the state of the system. The observality grammian reflects the ability of a state $\aleph$ to affect the output $\mathbf{y}$ of a system. In the case of a time invariant system, the stationary solutions of (13) are given by the Lyapunov equations :

$$\mathbf{A}\cdot\mathbf{W_c} + \mathbf{W_c}\cdot\mathbf{A}^T + \mathbf{B}\cdot\mathbf{B}^T = 0 \qquad \mathbf{A}^T\cdot\mathbf{W_o} + \mathbf{W_o}\cdot\mathbf{A} + \mathbf{C}^T\cdot\mathbf{C} = 0 \quad (14)$$

The singular values of the Grammians product are invariant under linear transformation and are called the Hankel singular values $\gamma_i = \sqrt{\lambda_i(\mathbf{W_c}\cdot\mathbf{W_o})} \quad i = 1 \ldots \mathbf{N}$.

The order $\mathbf{N}$ of the nodal representation can become very huge when the number of degrees of freedom of the finite element model is very large. A convenient approach is to use a modal representation. Defining the state variables as the modal displacement and velocities :

$$\aleph = \begin{Bmatrix} \mathbf{x}_m \\ \dot{\mathbf{x}}_m \end{Bmatrix} \quad (15)$$

the modal state-space form is then defined by the following triple :

$$\mathbf{A} = \begin{bmatrix} 0 & \mathbf{I} \\ -\Omega^2 & -2\cdot\mathbf{Z}\cdot\Omega \end{bmatrix} \quad \mathbf{B} = \begin{bmatrix} 0 \\ \mathbf{B}_m \end{bmatrix} \quad \mathbf{C} = \begin{bmatrix} \mathbf{C}_{mx} & \mathbf{C}_{mx} \end{bmatrix} \quad (16)$$

where $\Omega = \mathbf{diag}(\omega_1, \omega_2, \ldots \omega_n)$ is natural frequencies matrix associated with the $(n \times n_m)$ modal matrix $\Phi = \begin{bmatrix} \Phi_1 & \Phi_2 & \ldots & \Phi_{n_m} \end{bmatrix}$. The modal mass, damping (assuming proportional damping for convenience) and stiffness diagonalized matrix are obtained by the modal projection on $\mathbf{K}$, $\mathbf{D}$, $\mathbf{M}$:

$$\mathbf{M}_m = \Phi^T \cdot \mathbf{M} \cdot \Phi \quad \mathbf{D}_m = \Phi^T \cdot \mathbf{D} \cdot \Phi \quad \mathbf{K}_m = \Phi^T \cdot \mathbf{K} \cdot \Phi$$
$$\mathbf{Z} = \frac{1}{2} \cdot \mathbf{M}_m^{-1} \cdot \mathbf{D}_m \cdot \Omega^{-1} \qquad (17)$$

In the same way, the modal input, displacement and velocity outputs matrices are introduced by :

$$\mathbf{B}_m = \mathbf{M}_m^{-1} \cdot \Phi^T \cdot \mathbf{B}_0 \quad \mathbf{C}_{mx} = \mathbf{C}_{0x} \cdot \Phi \quad \mathbf{C}_{m\dot{x}} = \mathbf{C}_{0\dot{x}} \cdot \Phi \qquad (18)$$

The dimension of this modal state-space representation $(2 \cdot \mathbf{n}_m \times 2 \cdot \mathbf{n}_m)$ is then more economic than the nodal state-space representation $(2 \cdot \mathbf{n} \times 2 \cdot \mathbf{n})$ since $\mathbf{n}_m << \mathbf{n}$. An other important advantage of the modal state representation is that the resulting controllability and observability Grammians are diagonally dominant (see Gawronski) :

$$\mathbf{W}_c \cong \mathrm{diag}(w_{ci} \cdot \mathbf{I}_{2\times 2}) \quad \mathbf{W}_o \cong \mathrm{diag}(w_{oi} \cdot \mathbf{I}_{2\times 2}) \qquad (19)$$

Diagonal entries of (19) and Hankel singular values are then obtained as follows :

$$w_{ci} = \frac{\|\mathbf{B}_{mi}\|_2^2}{4 \cdot \zeta_i \cdot \omega_i} \quad w_{oi} = \frac{\|\mathbf{C}_{mi}\|_2^2}{4 \cdot \zeta_i \cdot \omega_i} \quad \gamma_i \cong \frac{\|\mathbf{B}_{mi}\|_2 \cdot \|\mathbf{C}_{mi}\|_2}{4 \cdot \zeta_i \cdot \omega_i} \qquad (20)$$

Transfer function norms $\mathbf{H}_2, \mathbf{H}_\infty, \mathbf{H}_{hankel}$ serve as a measure of the controlling ability of an actuator / sensor configuration applied on a system defined by $(\mathbf{A}, \mathbf{B}, \mathbf{C})$. In this paper, only $\mathbf{H}_2$ norm will be considered. The transfer function of this system is given by :

$$\mathbf{G}(\omega) = \mathbf{C} \cdot (\mathbf{j} \cdot \omega \cdot \mathbf{I} - \mathbf{A})^{-1} \cdot \mathbf{B} \qquad (21)$$

The $\mathbf{H}_2$ norm of the transfer function is defined by :

$$\|\mathbf{G}\|_2 = \frac{1}{2 \cdot \pi} \cdot \int_{-\infty}^{+\infty} \mathrm{tr}\left(\mathbf{G}^*(\omega) \cdot \mathbf{G}(\omega)\right) d\omega = \mathrm{tr}\left(\mathbf{C}^T \cdot \mathbf{C} \cdot \mathbf{W}_c\right) = \mathrm{tr}\left(\mathbf{B} \cdot \mathbf{B}^T \cdot \mathbf{W}_o\right) \qquad (22)$$

For flexible systems in the modal state representation, $\mathbf{H}_2$ norm can be expressed in terms of the norms of the modes. This modal decomposition affords then a visibility on each modal contributions. Taking the transfer function of the i^{th} mode :

$$\mathbf{G}_i(\omega) = \mathbf{C}_i \cdot (\mathbf{j} \cdot \omega \cdot \mathbf{I} - \mathbf{A}_i)^{-1} \cdot \mathbf{B}_i \qquad (23)$$

the $\mathbf{H}_2$ norm of the i^{th} mode can be estimated (see Gawronski) by :

$$\|\mathbf{G}_i\|_2 \cong \frac{\|\mathbf{B}_i\|_2 \cdot \|\mathbf{C}_i\|_2}{2 \cdot \sqrt{\zeta_i \cdot \omega_i}} = \frac{\|\mathbf{B}_i\|_2 \cdot \|\mathbf{C}_i\|_2}{\sqrt{\Delta\omega_i}} \cong \gamma_i \cdot \sqrt{2 \cdot \Delta\omega_i} \qquad (24)$$

with $\Delta\omega_i = 2 \cdot \zeta_i \cdot \omega_i$ is the half-power frequency at the i^{th} resonance. By (22) and since the Grammians are diagonally dominant in the modal state-space representation, the $\mathbf{H}_2$ norm of the complete system is estimated by the *rms* sum of the modal norms :

$$\|\mathbf{G}\|_2 \cong \sqrt{\sum_{i=1}^{n_m} \|\mathbf{G}_i\|_2^2} \qquad (25)$$

Equations (24) and (25) are the bases of a selection strategy for actuator and sensor placement.

The procedure starts with the selection of the best actuators position. Assuming that all degrees of freedom are monitored, we compute the placement index σ_{2ki} that evaluates the importance of the k^{th} actuator at the i^{th} mode on the global transfer function $\mathbf{H}_2$ norm :

$$\sigma_{2ki} = w_{ki} \cdot \frac{\|\mathbf{G}_{ki}\|_2}{\|\mathbf{G}\|_2} \qquad (26)$$

where w_{ki} is an user weight reflecting the accorded importance on the mode and the actuator in application. A placement indices matrix can then be constructed by varying $\mathbf{B}_0$ and with $\mathbf{C}$ fixed :

$$\Sigma_2 = \begin{bmatrix} \sigma_{211} & \cdots & \sigma_{21n} \\ \vdots & \ddots & \vdots \\ \sigma_{2n_m1} & \cdots & \sigma_{2n_mn} \end{bmatrix} \begin{array}{l} \Leftarrow i^{th} mode \\ \\ \Uparrow \\ k^{th} actuator \end{array} \qquad (27)$$

which clearly shows the ability of the k^{th} actuator position to affect the i^{th} mode. Once the actuator positions selected ($\mathbf{B}_0$ optimized), the same procedure can be repeated by constructing a sensor placement indices matrix, helping the selection of the best sensors positions.

Illustrative example : experimental modal analysis on a clamped free plate

As an illustrative example, a 0.16 x 0.08 x 0.001 m clamped-free stainless steel plate, fitted with one commercial piezoelectric (PZT) laminate on each face where studied. These two piezoelectric laminates

are placed near the clamped side of the plate. The first step is to perform a finite element model. This model uses volumic finite elements. The poor efficiency when meshes don't approach the cubic shape is the main drawback of this kind of elements. The five computed eigen-frequencies were estimated at :

- 33 Hz : first flexion mode,
- 168 Hz : first mode of torsion,
- 206 Hz : second mode of flexion,
- 529 Hz : second mode of torsion,
- 569 Hz : third mode of flexion.

Figure 1 presents the finite element mesh of the experiment. The support plate is discretized in 918 mechanical degrees of freedom. The two laminates are discretized in 90 mechanical degrees of freedom and 1 electrical potential for each electrodes.

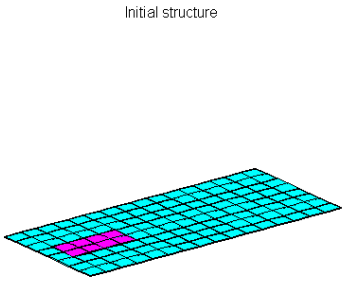

Figure 1 : *FEM plate meshing*

The second step of the procedure begins with the selection of the best actuator position using (27). Figure 2 shows a graphical representation of the actuator placement indices for the 5 targeted modes.

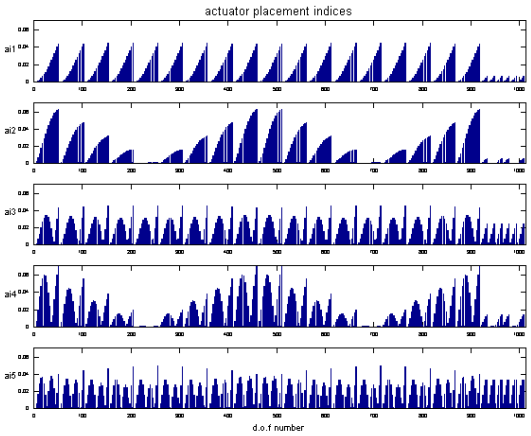

Figure 2 : *Actuator placement indices*

As expected, controllability of actuator position is best at the two corners, situated at the opposite of the clamping side. Direction of excitation is of course perpendicular to the plate.

Once selected the excitation point, the sensor placement indices matrix have also been constructed for the selection of the best sensor positions (see figure 3). As for the excitation selection, the best sensor position are given at the plate corner.

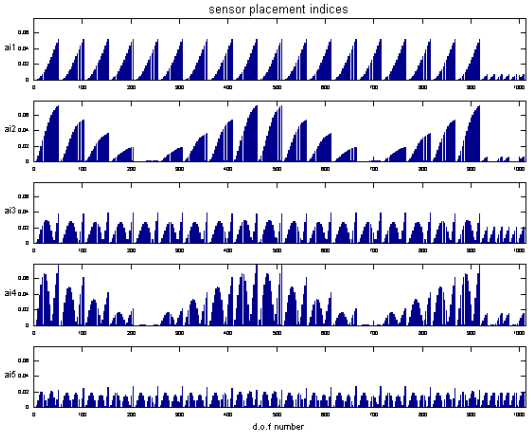

Figure 3 : *Sensor placement indices*

In order to increase the visibility in the case of graphical animation, the 32 sensor locations have been equally spaced on the plate.

FRFs (accelerometers/force and laminates responses/force) have then been monitored by exciting the structure by means of an impulse hammer (see figure 4).

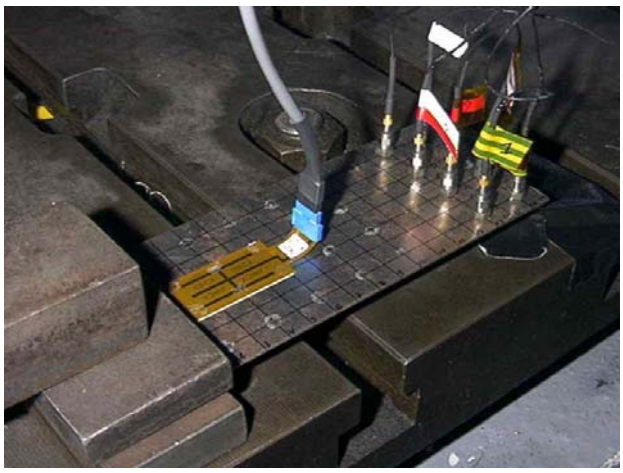

Figure 4 : *Experimental set-up*

Due to the light weight of the structure, the accelerometer masses have disturbed the ***FRF***s curves. Non-contact measurements, by means of a LASER vibrometer, have then been preferred. Modal extraction with a classical circle fitting algorithm (see Maia, Silva and al.) have then been performed on ***FRF***s measurement. Figure 5 presents the achieved modal identification.

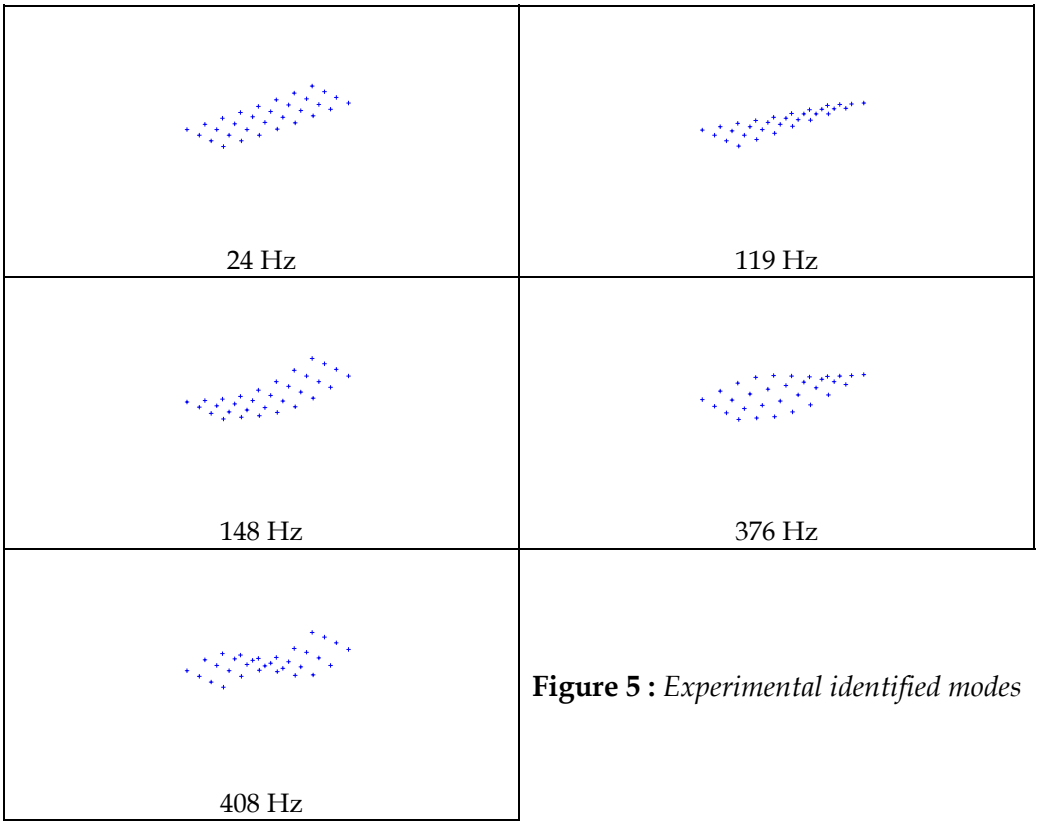

Figure 5 : *Experimental identified modes*

Model updating : theory and application on experimental data

In the previous chapters, we have seen how to choose optimal actuator and sensor locations and how to perform modal analysis on piezoelectric structures. In this chapter, we will attempt to improve an initial finite element model so to fit experimental data with modelling results.

Iterative, sensitive methods are very popular in the model updating community. These methods are based on the minimisation of a residue vector expressing the difference between the experimental data and modelling results. A combination of resonance frequency differences and frequency response function is favourable in most cases (see Heylen and al.).

Resonant frequencies sensitivities are based on the first order terms of a Taylor expension :

$$\omega_{X\,j}^2 = \omega_{A\,j}^2 + \sum_{i=1}^{N_p} \frac{\partial \omega_{A\,j}^2}{\partial p_i} \cdot p_i \qquad (28)$$

where p_i is the i^{th} updating parameters $(1 \ldots N_p)$,

$\omega_{X\,j}$ is the j^{th} experimental resonant pulsation.

$\omega_{A\,j}$ is the j^{th} corresponding analytical resonant pulsation associated with the mode $\phi_{A\,j}$, solution of :

$$K_A \cdot \phi_{A\,j} = \omega_{A\,j}^2 \cdot M_A \qquad (29)$$

By differentiating (29) versus p_i, and assuming no structural damping, it is possible to develop the eigenvalues sensitivities by :

$$\frac{\partial \omega_{A\,j}^2}{\partial p_i} = \frac{\phi_{A\,j}^T \cdot \left(\frac{\partial K_A}{\partial p_i} - \omega_{A\,j}^2 \cdot \frac{\partial M_A}{\partial p_i} \right) \cdot \phi_{A\,j}}{\phi_{A\,j}^T \cdot M_A \cdot \phi_{A\,j}} \qquad (30)$$

In the same way, the difference frequency response function of the system to an excitation at point k is given by :

$$G_A(\omega) \cdot \sum_{i=1}^{N_p} \left(\frac{\partial K_A}{\partial p_i} - \omega^2 \cdot \frac{\partial M_A}{\partial p_i} \right) \cdot \{G_X(\omega)\} = \{G_A(\omega)\}_k - \{G_X(\omega)\} \qquad (31)$$

where $\mathbf{G_A}(\omega) = \left(\mathbf{K_A} - \omega^2 \cdot \mathbf{M_A}\right)^{-1}$ is the global matrix of analytical transfer functions at pulsation ω,

$\{\mathbf{G_A}(\omega)\}_k$ is the k^{th} column of $\mathbf{G_A}(\omega)$,

$\{\mathbf{G_X}(\omega)\}$ is the experimental vector of frequency response function of the structure submitted to a force applied on the k^{th} degree of freedom.

Inevitability, there will be an incompatibility between the size of the finite element model and the size of experimental data : the number of degrees of freedom of the model most often exceeds the number of measured degrees of freedom. Matching can be made by experimental data expansion or model reduction. Literature presents various solution (see Maia and al. or Heylens and al.). In this paper, the dynamic reduction is used since it gives an exact representation of the system at a given pulsation ω_{test}.

The system formed by equation (28) and (31) for the identified resonances $\omega_{X\,j}$ and at the tested frequencies ω_{tested} has generally to be solved by least square technique (since the number of relations is generally not equal to the number of updating parameters $\mathbf{p}_i$). The choice of the updated parameters is very important and not straightforward : bad parameters choice could give a solution which is acceptable on a mathematical point of view but not physically realist. Moreover, in the case of piezoelectric structure, the orders of magnitudes of the different coupling matrices are very spread : $\mathbf{K} \div 10^{10}$, $\mathbf{\Theta^s} \div 10^{0}$ and $\mathbf{C_p} \div 10^{-10}$. This numerical ill-conditioning requires then some cares when matrix inversions are required :

- at the model matching level,
- at the resolution of the least square problem.

Singular value decomposition could be then used to improve these steps. For example, a matrix $\mathbf{A}$ can be factored as $\mathbf{A} = \mathbf{U} \cdot \mathbf{\Sigma} \cdot \mathbf{V}^t$ where $\mathbf{U}$ and $\mathbf{V}$ are orthogonal matrices which contain the left and right singular vectors and $\mathbf{\Sigma}$ is a diagonal matrix that contains the singular values σ_i of $\mathbf{A}$. Some singular values σ_i will tends to zeros if some rows of $\mathbf{A}$ are not totally independent. A criterion of rejection could be then established to reject small singular values by comparing them, for example, to a threshold proportional to the singular values average :

$$\sigma_{threshold} = 10^{-th} \cdot \frac{1}{\mathbf{N}} \cdot \sum_{i=1}^{N} \sigma_i \qquad (32)$$

where $\mathbf{th}$ is an user defined integer.

A model updating procedure has then been applied on the finite element model of the piezoelectric plate described in the previous section. Figure 6 presents the experimental ***FRF***s; dashed lines point the selected frequencies for the updating (note also, on the top, the monitored signal of the two piezoelectric elements).

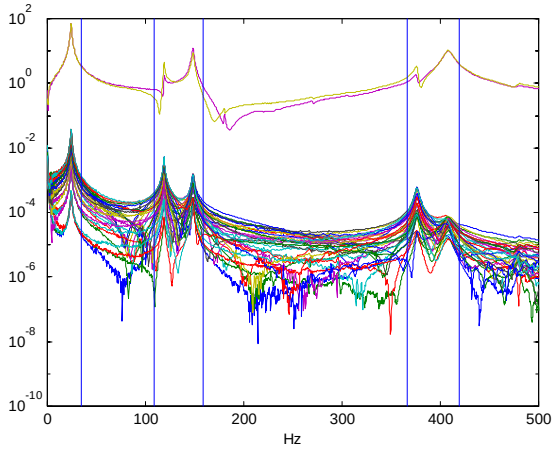

Figure 6 : *Experimental **FRF**s*

The correction procedure have also been performed on the five resonance frequencies identified during experimental modal analysis. The number of updating parameters has been carefully chosen : the Young modulus and shear coefficients of the plate material and piezo-laminates material have been taken into account. Moreover, a correction on the piezoelectric global electromechanical coupling matrices have been performed independently on each laminates. Figure 7 presents graphically the achieved model corrections.

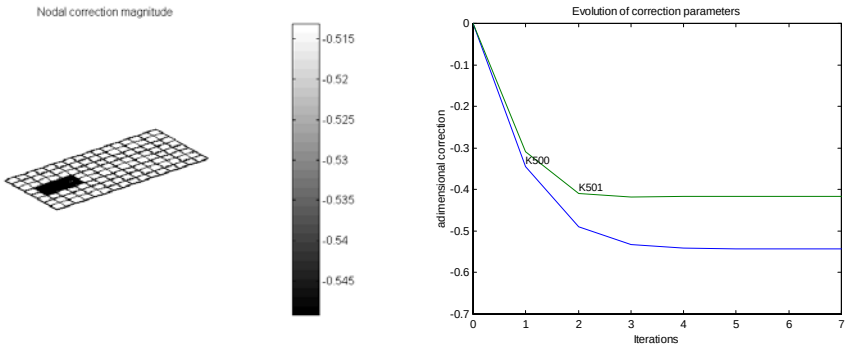

Figure 7 : *Mechanical (on left) and piezoelectric (on right) model correction*

It can be seen that correction differences appears between the two piezoelectric laminates, as expected with the gap existing between the two laminates responses visible on figure 6.

Finally, figure 8 shows the comparison between the experimental modes and the updated system modes by means of the extensively used *Modal Assurance Criterion* (MAC) which is defined as follows :

$$MAC(\phi_{X_i}, \phi_{A_j}) = \frac{\left|\phi_{X_i}^T \cdot \phi_{A_j}\right|^2}{\left(\phi_{X_i}^T \cdot \phi_{X_i}\right) \cdot \left(\phi_{A_j}^T \cdot \phi_{A_j}\right)} \qquad (33)$$

The MAC always lies between 0 (no correlation between modes) and 1 (modes are perfectly correlated). Figure 8 shows a very good achieved correlation but resonant frequencies of mode 3 and 5 are not perfectly fitted with the experimental identified eigen-frequencies.

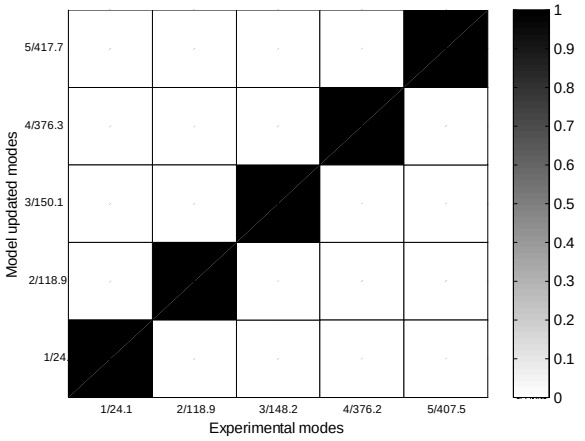

Figure 8 : *MAC matrix between experimental and model updated modes*

Conclusion

The described method for the identification of a piezoelectric system has been applied on an experimental case. Based on the observability and controllability Grammians, the procedure begin by the selection of the best excitation and sensing points in order to ensure a good experimental identification. Modal extraction performed, an initial finite element model is improved by using the sensitivities on eigen-frequencies and ***FRF***s. Achieved results are very encouraging but could be certainly more improved by a better selection of udpating parameters.

Acknowledgement

This work has been sponsored by the *Région Wallonne* of Belgium.

References

1. Maia, Silva and al., *Theoretical and experimental modal analysis*, Research Studies Press LTD., 1997.

2. Saunders, W.R., Cole, D.G., Robertshaw, H.H., Experiments in piezostructure modal analysis for MIMO feedback control, *Smart Mater. Struct.*, 1994, **3**, 210-218.

3. Géradin, M., Rixen, D., *Mechanical vibrations, Theory and application to structural dynamics*, Wiley, 1993.

4. Kammer, D.C., Sensor placement for on-orbit modal identification and correlation of large space structures, *Journal of Guidance Control and Dynamics*, **14**, 251-259.

5. Gawronski, W.K., *Dynamics and control of structures : a modal approach*, Springer, 1998

6. Kwakernaak, H.K., Sivan, R., *Linear optimal control systems*, Wiley, 1972

7. Heylen, W., Lammens, S., Sas, P., *Modal analysis theory and testing*, K.U. Leuven, PMA, 1998